Mechanical Manipulation Assisted Self-Assembly To Achieve Defect Repair and Guided Epitaxial Growth of Individual Peptide Nanofilaments

Fu-Chun Zhang,[†,‡] Feng Zhang,[†] Hai-Nan Su,[†] Hai Li,[†] Yi Zhang,[†,*] and Jun Hu[†,*]

[†]Shanghai Institute of Applied Physics, Chinese Academy of Sciences, Shanghai 201800, China, and [‡]Graduate School of the Chinese Academy of Sciences, Beijing 100039, China

ABSTRACT We have succeeded in the production of defect-free and spatially organized individual one-dimensional peptide nanofilaments by real-time control of the self-assembly process on a solid substrate. Using a unique mechanical manipulation method based on atomic force microscopy, we are able to introduce mechanical stimuli to generate active ends at designated positions on an existing peptide nanofilament previously formed. By doing so, defects in the filament were removed, and self-repairing occurred when the active ends extended along the direction of the supporting lattice, resulting in the closure of the broken filament. Furthermore, new active ends of the nanofilaments can be specifically generated to guide the self-assembly of new filaments at designated positions with selected orientations. The mechanism of defect repair and guided epitaxial growth is also discussed.

KEYWORDS: peptide nanofilament · self-assembly · mechanical manipulation · defect repair · guided epitaxial growth

The generation of defect-free one-dimensional (1-D) nanostructures[1,2] on inorganic solid substrates with controlled spatial organization[3−8] is a continuing challenge and calls for new concepts. Since most nanodevices are composed of one or a few 1-D nanostructures, it is important to ensure that imperfect structures or defects are not present in those structures. To the best of our knowledge, little progress has been made on the real-time monitoring and correction of defects in individual 1-D nanostructures during their formation. On the other hand, great effort has been directed toward the development of novel methods for spatial organization of 1-D nanomaterials on surfaces,[3−8] but very few procedures exist that can site-specifically fabricate individual, properly oriented 1-D nanomaterials with high spatial resolution. Herein, we address these concerns through manipulation of individual peptide nanofilaments during peptide self-assembly on a substrate, with monitoring of its progress and repair of defects *in situ* and with control of the growth process in a serial manner from the nanometer to the micrometer scale.

Our strategy was inspired by nature. In a biological system, molecular assembly starts or terminates in response to chemical or biological stimuli at the right place and the right time. If any errors are present during the assembly, nature has developed mechanisms to recognize and correct errors by introducing error proof-reading and self-repair processes, usually with the participation of enzymes. In principle, if one can introduce suitable physical stimuli (*e.g.*, mechanical force) *in situ* into a self-assembly process at the molecular level, similar mechanisms as those found in enzymatic machinery can be achieved. Recent developments in atomic force microscope (AFM)-based mechanical manipulation[9−13] have provided the potential for such physical stimuli. For example, through the application of a mechanical force from a tapping AFM tip, it has been reported that peptide-assembled nanostructures are broken into fragments, which in turn serve as nucleation seeds for further assembly.[14]

We applied this strategy to the self-assembly of peptides to generate 1-D nanobiomaterials. The 1-D nanomaterials self-assembled from peptides and proteins are characterized by biocompatibility, chemical flexibility, and biological recognition abilities,[15−20] which makes them well-suited for many potential applications, such as for nanofluidic device,[21] fabrication of metallic nanowires,[22,23] scaffolds of tissue,[24,25] drug delivery,[26] and biosensers.[27,28] The self-assembly of peptides is assumed to include two steps: nucleation seed formation and

*Address correspondence to zhangyi@sinap.ac.cn, junhu22@hotmail.com.

Received for review July 7, 2010 and accepted September 02, 2010.

Published online September 14, 2010.
10.1021/nn101541m

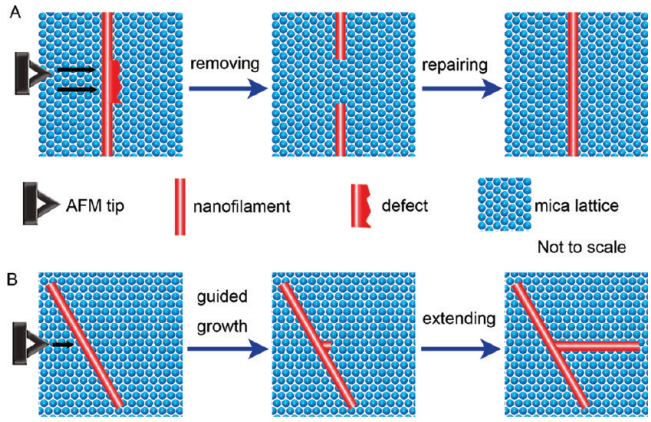

Figure 1. Schematic drawing indicating repair of a broken nanofilament (A) and the formation of "active ends" by AFM mechanical manipulation and subsequent extension of a new nanofilament (B). (A) After removing a defective part of a nanofilament by AFM raster scanning once in the selected region with sufficient load, a nanogap with two active ends was created on a nanofilament, which was subsequently repaired. In this case, by increasing the peptide concentration in the bulk solution, the active ends extended until a final closure of the nanogap. (B) After the AFM tip scanned a single line with sufficient load at the direction indicated with the black arrow, a new active end was created beside an existing nanofilament, which further served as a new nucleation seed for extension of a long oriented nanofilament.

1-D nanofilament growth. After nucleation seeds have formed, and if their ends are active, peptide monomers can add to the seeds to extend the peptide nanofilaments. In particular, the orientations of the growing 1-D peptide nanofilaments on solid substrates can be precisely controlled by the underlying lattice of the substrate through an "epitaxial" process.[29−33]

In our studies, we used the GAV-9 peptide,[34,35] NH_2-VGGAVVAGV-$CONH_2$, a conserved consensus of three neurodegenerative disease related proteins: α-synuclein, amyloid β protein, and prion protein.[36] In previous studies, we determined the self-assembly behavior of peptides at water−solid interfaces[34] and observed the diffusion and self-assembly in ambient water nanofilms on mica.[35] Here, by using a unique mechanical manipulation carried out with an AFM recently developed in our laboratory,[9] we have successfully created "active ends" at designated positions on a peptide nanofilament previously formed on the substrate. The created "active ends" are analogous to nuclear seeds for either the repair of broken nanofilaments on the surface (Figure 1A) or growing extra nanofilaments at the selected positions with new growth orientations along the underlying lattice (Figure 1B).

RESULTS AND DISCUSSION

Defect Repair. AFM study enabled us to monitor the peptide self-assembly process. This crucial procedure allowed us to find errors in the self-assembly process and to effect *in situ* repair of the defective parts of the 1-D nanostructures in real-time. The GAV-9 molecule is able to self-assemble into uniform 1-D nanofilaments in three preferred orientations along the mica lattice when the monomer concentration is higher than critical monomer concentration (1.6 mM).[34] However, defects that represent inhomogeneous parts of a nanofilament can also appear (Figure 2A). By employing an AFM mechanical manipulation method, the defective part could be excised immediately and repaired *in situ*. For example, raster scanning with the AFM tip once with a load in the selected region removed the defective parts, resulting in a large gap ~700 nm in size and exposing two ends (Figure 2B). In our experiment, AFM manipulation was usually carried out with a vertical load greater than a threshold force of ~4 nN. A vertical load less than 4 nN would not be sufficient to generate gaps on the nanofilaments. During AFM operation, the monomer concentration was less than 1.0 mM. At such a concentration, the self-assembly process was stopped; for example, no new nucleation seeds formed and the nanofilament did not extend. When the monomer concentration was increased to 1.0−1.6

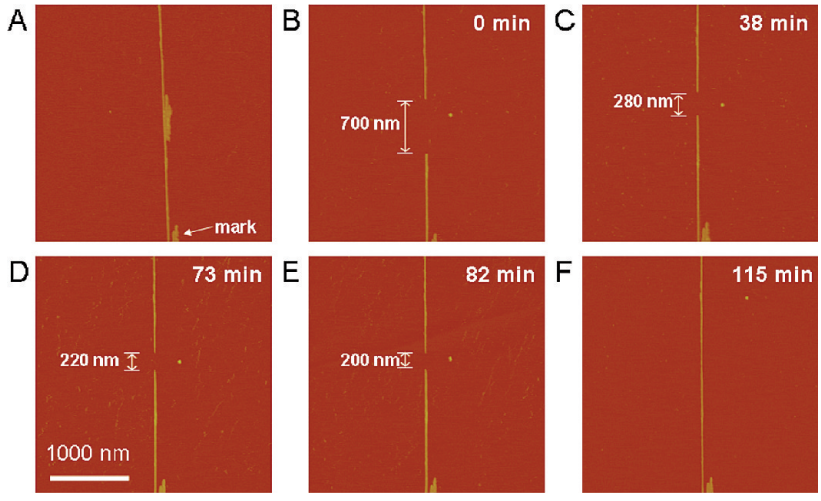

Figure 2. Tapping-mode AFM images of a GAV-9 nanofilament indicating the repair process of the filament after removal of a defect by AFM mechanical manipulation. (A) Original GAV-9 filaments in a solution with a low monomer concentration. A defective part appears in the middle region. The arrow points to featured filaments that serve as a mark to indicate that the repair happened in a same area. (B) Gap of 700 nm appeared after AFM removed the defective part. (C−F) When the monomer concentration increased, the GAV-9 molecules filled the gaps until continuous filaments were formed. The scale bar in panel D is 1000 nm and applies to all images.

mM, the peptide self-assembly was restored and the two exposed active ends could extend along its original direction until the two ends merged (see Figure 2B−F, showing a typical "repairing" process). Interestingly, the extending rates of the two newly generated active ends may be very different.[34,37] In the case of Figure 2, the upper active end extended about 50, 40, and 20 nm, respectively, from Figure 2B to 2C, C to D, and D to E, while in the same time periods, the bottom one extended about 370, 20, and 0 nm, respectively. It should be emphasized that from AFM studies the configuration of the freshly formed nanofilaments shows no detectable difference than that of the nanofilaments formed previously. We infer that the molecular arrangement in active ends is similar to that on nanofilament (*i.e.*, antiparallel β sheet with an upright orientation).[34]

The manipulation to generate the active ends is quite subtle. We found that the repair of the peptide nanofilament may not always result in closure of mechanically broken gaps. We speculated that one or both of the active ends were slightly moved during the AFM operation, which led to the mismatch after their extension. This kind of mismatch can be avoided by utilizing a special AFM manipulation protocol, in which the AFM tip first cut the nanofilament on the two sides of a defect with two independent cutting operations, followed by raster scanning at the isolated defect with sufficient load to remove it. By following this protocol, we repaired in total 21 gaps that were generated on uniform nanofilaments by AFM mechanical manipulation, a successful rate of 100% from the data we currently have.

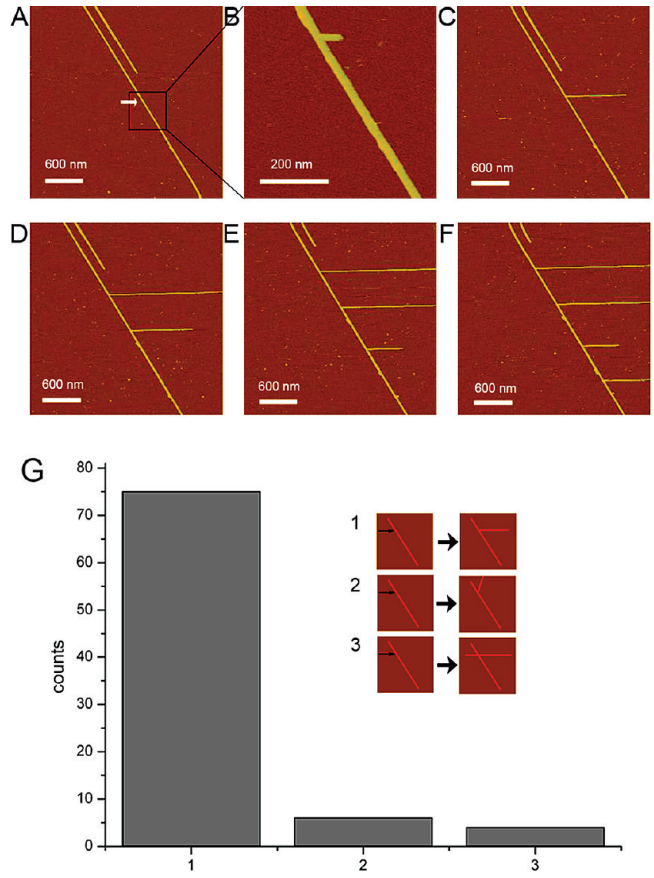

Figure 3. Series of tapping-mode AFM images of GAV-9 nanofilaments indicating the position-guided epitaxial growth of individual peptide nanofilaments. (A) Original GAV-9 nanofilaments. The position of a nanofilament was manipulated by the AFM tip by pushing it toward the direction indicated with the white arrow. (B) Active end was created by AFM manipulation as evidenced by the presence of a new short nanofilament at the side of the original one. (C) Extending of the new nanofilament. (D−F) By repeating the AFM manipulation three times at selected positions on the original nanofilament, three more active ends were generated and they extended to long filaments. (G) Histogram showing that the success rate of position-guided epitaxial growth of peptide nanofilaments can be ~90%. The insets in panel G indicate the correct (1) and two unexpected (2 and 3) growth behaviors of new nanofilaments generated by the AFM mechanical manipulation.

As discussed previously,[34] the self-assembly of GAV-9 peptide on mica surface is driven by the hydrophobic interaction and hydrogen bond between the peptide molecules as well as the electrostatic interaction between negatively charged mica substrate (because of the detachment of the potassium ions from the surface) and positively charged peptide N-terminus. The hydrophobic interaction and hydrogen bond are the origin of the self-assembly of the peptide into nanofilaments, while the electrostatic interaction guides the nanofilaments to extend to some preferred orientations on the mica surface. In this paper, AFM mechanical manipulation provides controlled mechanical energy to break the above-mentioned weak interactions in the peptide self-assembling system and site-specifically generates active ends for defect repair of the nanofilaments.

Guided Epitaxial Growth. Since the active ends could be moved during the AFM operation, we expected that the finely controlled mechanical manipulation would also be used to induce the formation of active ends on an existing nanofilament at designated positions and guide the filament extension at a selected orientation along the underlying mica lattice. Figure 3 illustrates a good example of the dynamic process of AFM mechanical manipulation guided epitaxial growth of individual nanofilaments. After pushing on a nanofilament at a single scanning line along the direction and position indicated with the white arrow in Figure 3A, a branch with an active end appeared at one side of the nanofilament (Figure 3B), which served as the nucleation seed and extended gradually into a new nanofilament (Figure 3C). Here the orientation of the new nanofilament followed the AFM pushing direction, which had an angle of 60° (or 120°) with respect to the original nanofilament and coincided with the mica lattice. If

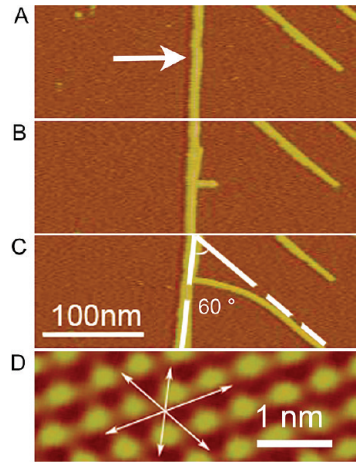

Figure 4. Tapping-mode AFM images indicating the extension of a nanofilament guided by the AFM tip with a direction not matching the orientation of the underlying mica lattice. (A) Original nanofilament was manipulated by the AFM tip along the direction indicated by the arrow. (B) New filament was created by the AFM mechanical manipulation. The filament induced by the AFM operation is oriented at 90° to the original nanofilament. (C) Finally, the new nanofilament extended in the same direction as the lattice. (D) Contact-mode AFM image of mica substrate. Image D was taken in pure water, which was subsequently replaced with GAV-9 peptide solution for the growth of the peptide nanofilaments shown in images A−C. The arrows indicate the lattice orientations.

the pushing direction did not match with the mica lattice (*e.g.*, perpendicular to the original peptide nanofilament), an active end first appeared along the AFM tip pushing direction (Figure 4A). However, the newly formed nanofilament is in a mesostable state, and its elongation finally pointed toward the mica lattice direction, which is in the minimal energy state[38] (Figure 4B,C). We also found that pushing at a single AFM scanning line on a nanofilament was sufficient for generating a new nucleation seed at the side of the nanofilament. Raster scanning of a part of the nanofilament with a large load may result in multiple active ends at the sides of the nanofilament and subsequently may generate multiple nanofilaments from the expected site in an uncontrollable manner, a phenomenon similar to the one reported by Yang *et al.*[14] During AFM pushing, the vertical load applied by the AFM tip is estimated to be ~10 nN according to Hooke's law, which is much larger than the force that is used normally in tapping-mode imaging in liquids. Interestingly, the peptide concentration during this process is lower than the critical aggregation concentration, typically 1.3 mM, which indicates that nanofilaments can extend even at less than critical concentrations once the active ends have been created.

The generation of new nanofilaments by using AFM mechanical manipulation is very convenient and repeatable. As shown in Figure 3D−F, three additional parallel nanofilaments with almost the same separation were fabricated after three "pushing" operations by the AFM tip. The success rate can be ~90% (1 in Figure 3G). Two kinds of unexpected results were found in a series of repeated experiments. In one case, newly formed nanofilaments were extending with an angle of 60° relative to the AFM pushing direction (2 in Figure 3G). In the other case, newly formed nanofilaments elongated bidirectionally (3 in Figure 3G). Nanofilament growth in other directions in these experiments was not found. Nevertheless, since AFM mechanical manipulation has high spatial resolution, and the extension of a new nanofilament is along the direction of the mica lattice, this method allows us to precisely control the position and orientation of a new nanofilament by employing AFM mechanical manipulation generated active ends, monitoring and controlling the nanofilament growth process *in situ*.

We investigated how the active ends were formed under AFM mechanical manipulation. Since the monomer concentration is less than the critical aggregation concentration, it is not likely that these active ends are from the nucleation seeds that are randomly deposited on the mica surface from the GAV-9 solutions. We also eliminated the possibility that the contact site of the AFM tip with the mica surface serves as a nucleation seed because control experiments conducted on the bare mica did not generate any active ends. We speculated that the AFM mechanical manipulation provides sufficient mechanical energy to break the electrostatic interaction between the substrate and the peptide, resulting in removal and rearrangement of some peptide molecules at planned positions and formation of active ends that are capable of extending to form a new nanofilament. This hypothesis was supported by experimental results shown in Figure 5, which indicates that a small part of the nanofilament was moved and pointed in the AFM pushing direction, serving as a new active end. Most of the active ends should point in the pushing direction since >90% of newly formed nanofilaments are oriented in this direction.

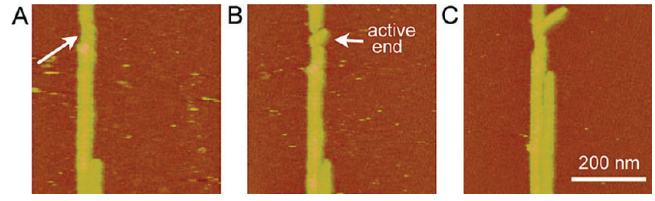

Figure 5. Tapping-mode AFM images revealing the detailed process of AFM-guided epitaxial growth of peptide nanofilaments. (A) Original nanofilament was pushed by the AFM tip once along the direction indicated by the white arrow. (B) Original nanofilament was broken by the AFM mechanical manipulation, and in the meantime, a small part of the nanofilament was moved and pointed in the AFM pushing direction, serving as a new active end (indicated with a white arrow) for nanofilament extension. (C) Active end extended along the lattice direction and a new nanofilament formed. At the same time, the gap on the original nanofilament was closed. The scale bar in panel C is 200 nm and applies to all images.

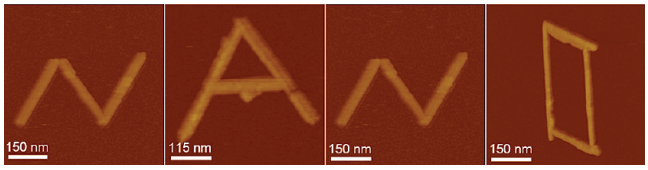

Figure 6. Tapping-mode AFM images showing the word "NANO" composed of individual GAV-9 nanofilaments.

Pattern Generation. By combining the AFM mechanical manipulation methods mentioned above, patterns of peptide nanofilaments can be generated. For example, a pattern with the word "NANO" was formed on the solid substrate (Figure 6). We emphasize that our method is based on the local manipulation of the self-assembly of the peptide, which enables us to control in real-time the growth of individual nanofilaments. Our method is distinguished from the strategy that synthesizes nanowire superstructures through the change of synthesis condition in bulk[39] and provides more operational freedom in nanofabrication that would result in more complicated patterns. With the development in the automation of the AFM manipulation process and the application of arrayed AFM tips,[40] the efficiency of our current manipulation method would be dramatically increased.

CONCLUSIONS

In summary, we have presented an approach to produce spatially organized individual one-dimensional peptide nanofilaments by delicately manipulating the peptide self-assembly process on solid substrates. When a defective site of a nanofilament is removed by AFM mechanical manipulation, active ends are generated and the peptide nanofilament repairs itself by filling in the gap with new GAV-9 molecules. An active end can also be generated on an existing nanofilament and pushed to the side of the nanofilament by AFM nanomanipulation. Subsequently, nanofilament extension at designated positions and selected orientations can also be achieved. Compared to previous publications,[14] our method offers more precise control on the position, direction, and shape of the newly formed peptide nanostructures and has the ability for defect repair. Importantly, this method may be extended to other monomers for fabricating individual 1-D nanostructures at selected locations and orientations on solid substrates if the monomer has a similar templating process in self-assembly on the substrate.

METHODS

GAV-9, NH_2-VGGAVVAGV-$CONH_2$, was synthesized with Boc solid-phase methodology and then was purified as described previously.[34] Before use, the powder of the GAV-9 peptide was dissolved into 10 mM PBS buffer (10 mM phosphate, 10 mM NaCl, pH 7.0). Muscovite mica ($KAl_2(Si_3AlO_{10})(OH)_2$, Sichuan Meifeng Co., China) was used as the inorganic substrate, which was freshly cleaved by adhesive tape prior to each experiment. GAV-9 nanofilaments were formed on the substrate as previously reported.[34]

All *in situ* AFM operations were performed on a commercial AFM (Nanoscope IIIa, Veeco/Digital Instruments) equipped with a J-scanner in a liquid cell. Silicon nitride cantilevers with a typical spring constant of 0.22 N/m (NPS, Veeco/Digital Instruments) were used. All AFM images were obtained with tapping-mode in liquid. During AFM imaging, to protect the sample, the force was applied as small as possible by adjusting the amplitude set point. To control the peptide self-assembly, the AFM manipulation procedure was conducted as shown in Figure 1. First, the AFM tip was located at positions of interest on a preformed nanofilament. Then the AFM tip was brought into contact with the substrate by setting a negative "lift height" in a "lift mode", which provides a quantitative mechanical force to manipulate the GAV-9 nanofilament at the desired locations. The vertical load can be roughly calculated from the cantilever's spring constant and the setting lift height that the tip had moved.[41] The nanofilaments can be either removed in part by the force or pushed to form an active end at the side for a new nanofilament. In this process, the GAV-9 monomer concentration was controlled either by addition of PBS buffer or GAV-9 solution of higher concentration (3.2 mM).

Acknowledgment. The authors thank Hua Bei and Xiuping Ren for helpful discussions. This work was supported by grants from Chinese Academy of Sciences (Nos. KJCX2.YW.H06 and KJCX2.YW.M03), the National Science Foundation of China (Nos. 10674147, 10975175, and 30600144), the National Basic Research Program of China (No. 2007CB936000), the Ministry of Health of China (2009ZX10004-301), and the Shanghai Municipal Commission for Science and Technology (0952 nm04600).

REFERENCES AND NOTES

1. Caroff, P.; Dick, K. A.; Johansson, J.; Messing, M. E.; Deppert, K.; Samuelson, L. Controlled Polytypic and Twin-Plane Superlattices in III−V Nanowires. *Nat. Nanotechnol.* **2009**, *4*, 50–55.
2. Wacaser, B. A.; Deppert, K.; Karlsson, L. S.; Samuelson, L.; Seifert, W. Growth and Characterization of Defect Free GaAs Nanowires. *J. Cryst. Growth* **2006**, *287*, 504–508.
3. Reches, M.; Gazit, E. Controlled Patterning of Aligned Self-Assembled Peptide Nanotubes. *Nat. Nanotechnol.* **2006**, *1*, 195–200.
4. Hill, R. J. A.; Sedman, V. L.; Allen, S.; Williams, P. M.; Paoli, M.; Adler-Abramovich, L.; Gazit, E.; Eaves, L.; Tendler, S. J. B. Alignment of Aromatic Peptide Tubes in Strong Magnetic Fields. *Adv. Mater.* **2007**, *19*, 4474–4479.
5. Huang, S. M.; Woodson, M.; Smalley, R.; Liu, J. Growth Mechanism of Oriented Long Single Walled Carbon Nanotubes Using "Fast-Heating" Chemical Vapor Deposition Process. *Nano Lett.* **2004**, *4*, 1025–1028.
6. Huang, Y.; Duan, X. F.; Wei, Q. Q.; Lieber, C. M. Directed Assembly of One-Dimensional Nanostructures into Functional Networks. *Science* **2001**, *291*, 630–633.
7. Kim, J. H.; Jung, Y.; Chung, J. W.; An, B. K.; Park, S. Y. Fabrication of a Patterned Assembly of Semiconducting Organic Nanowires. *Small* **2009**, *5*, 804–807.
8. Ural, A.; Li, Y. M.; Dai, H. J. Electric-Field-Aligned Growth of Single-Walled Carbon Nanotubes on Surfaces. *Appl. Phys. Lett.* **2002**, *81*, 3464–3466.
9. Hu, J.; Zhang, Y.; Gao, H. B.; Li, M. Q.; Hartmann, U. Artificial DNA Patterns by Mechanical Nanomanipulation. *Nano Lett.* **2002**, *2*, 55–57.

10. Xu, S.; Liu, G. Y. Nanometer-Scale Fabrication by Simultaneous Nanoshaving and Molecular Self-Assembly. *Langmuir* **1997**, *13*, 127–129.
11. Sugimoto, Y.; Pou, P.; Custance, O.; Jelinek, P.; Abe, M.; Perez, R.; Morita, S. Complex Patterning by Vertical Interchange Atom Manipulation Using Atomic Force Microscopy. *Science* **2008**, *322*, 413–417.
12. Hu, J.; Wang, M.; Weier, H.-U. G.; Frantz, P.; Kolbe, W.; Ogletree, D. F.; Salmeron, M. Imaging of Single Extended DNA Molecules on Flat (Aminopropyl)triethoxysilane-Mica by Atomic Force Microscopy. *Langmuir* **1996**, *12*, 1697–1700.
13. Liu, X. G.; Zhang, Y.; Goswami, D. K.; Okasinski, J. S.; Salaita, K.; Sun, P.; Bedzyk, M. J.; Mirkin, C. A. The Controlled Evolution of a Polymer Single Crystal. *Science* **2005**, *307*, 1763–1766.
14. Yang, H.; Fung, S. Y.; Pritzker, M.; Chen, P. Mechanical-Force-Induced Nucleation and Growth of Peptide Nanofibers at Liquid/Solid Interfaces. *Angew. Chem., Int. Ed.* **2008**, *47*, 4397–4400.
15. Vauthey, S.; Santoso, S.; Gong, H. Y.; Watson, N.; Zhang, S. G. Molecular Self-Assembly of Surfactant-like Peptides To Form Nanotubes and Nanovesicles. *Proc. Natl. Acad. Sci. U.S.A.* **2002**, *99*, 5355–5360.
16. Lashuel, H. A.; LaBrenz, S. R.; Woo, L.; Serpell, L. C.; Kelly, J. W. Protofilaments, Filaments, Ribbons, and Fibrils from Peptidomimetic Self-Assembly: Implications for Amyloid Fibril Formation and Materials Science. *J. Am. Chem. Soc.* **2000**, *122*, 5262–5277.
17. Matsumura, S.; Uemura, S.; Mihara, H. Fabrication of Nanofibers with Uniform Morphology by Self-Assembly of Designed Peptides. *Chem.—Eur. J.* **2004**, *10*, 2789–2794.
18. Wagner, D. E.; Phillips, C. L.; Ali, W. M.; Nybakken, G. E.; Crawford, E. D.; Schwab, A. D.; Smith, W. F.; Fairman, R. Toward the Development of Peptide Nanofilaments and Nanoropes as Smart Materials. *Proc. Natl. Acad. Sci. U.S.A.* **2005**, *102*, 12656–12661.
19. Aggeli, A.; Nyrkova, I. A.; Bell, M.; Harding, R.; Carrick, L.; McLeish, T. C. B.; Semenov, A. N.; Boden, N. Hierarchical Self-Assembly of Chiral Rod-like Molecules as a Model for Peptide β-Sheet Tapes, Ribbons, Fibrils, and Fibers. *Proc. Natl. Acad. Sci. U.S.A.* **2001**, *98*, 11857–11862.
20. Zhang, S. G. Fabrication of Novel Biomaterials through Molecular Self-Assembly. *Nat. Biotechnol.* **2003**, *21*, 1171–1178.
21. Adler-Abramovich, L.; Aronov, D.; Beker, P.; Yevnin, M.; Stempler, S.; Buzhansky, L.; Rosenman, G.; Gazit, E. Self-Assembled Arrays of Peptide Nanotubes by Vapour Deposition. *Nat. Nanotechnol.* **2009**, *4*, 849–854.
22. Scheibel, T.; Parthasarathy, R.; Sawicki, G.; Lin, X. M.; Jaeger, H.; Lindquist, S. L. Conducting Nanowires Built by Controlled Self-Assembly of Amyloid Fibers and Selective Metal Deposition. *Proc. Natl. Acad. Sci. U.S.A.* **2003**, *100*, 4527–4532.
23. Reches, M.; Gazit, E. Casting Metal Nanowires within Discrete Self-Assembled Peptide Nanotubes. *Science* **2003**, *300*, 625–627.
24. Ellis-Behnke, R. G.; Liang, Y. X.; You, S. W.; Tay, D. K. C.; Zhang, S. G.; So, K. F.; Schneider, G. E. Nano Neuro Knitting: Peptide Nanofiber Scaffold for Brain Repair and Axon Regeneration with Functional Return of Vision. *Proc. Natl. Acad. Sci. U.S.A.* **2006**, *103*, 7530.
25. Yokoi, H.; Kinoshita, T.; Zhang, S. G. Dynamic Reassembly of Peptide RADA16 Nanofiber Scaffold. *Proc. Natl. Acad. Sci. U.S.A.* **2005**, *102*, 8414–8419.
26. Lim, Y. B.; Lee, E.; Lee, M. Cell-Penetrating-Peptide-Coated Nanoribbons for Intracellular Nanocarriers. *Angew. Chem., Int. Ed.* **2007**, *46*, 3475–3478.
27. Yemini, M.; Reches, M.; Rishpon, J.; Gazit, E. Novel Electrochemical Biosensing Platform Using Self-Assembled Peptide Nanotubes. *Nano Lett.* **2005**, *5*, 183–186.
28. Yang, H.; Fung, S. Y.; Pritzker, M.; Chen, P. Ionic-Complementary Peptide Matrix for Enzyme Immobilization and Biomolecular Sensing. *Langmuir* **2009**, *25*, 7773–7777.
29. Whitehouse, C.; Fang, J. Y.; Aggeli, A.; Bell, M.; Brydson, R.; Fishwick, C. W. G.; Henderson, J. R.; Knobler, C. M.; Owens, R. W.; Thomson, N. H.; Smith, D. A.; Boden, N. Adsorption and Self-Assembly of Peptides on Mica Substrates. *Angew. Chem., Int. Ed.* **2005**, *44*, 1965–1968.
30. Hoyer, W.; Cherny, D.; Subramaniam, V.; Jovin, T. M. Rapid Self-Assembly of α-Synuclein Observed by *In Situ* Atomic Force Microscopy. *J. Mol. Biol.* **2004**, *340*, 127–139.
31. Brown, C. L.; Aksay, I. A.; Saville, D. A.; Hecht, M. H. Template-Directed Assembly of a *De Novo* Designed Protein. *J. Am. Chem. Soc.* **2002**, *124*, 6846–6848.
32. Yang, G. C.; Woodhouse, K. A.; Yip, C. M. Substrate-Facilitated Assembly of Elastin-like Peptides: Studies by Variable-Temperature *In Situ* Atomic Force Microscopy. *J. Am. Chem. Soc.* **2002**, *124*, 10648–10649.
33. Kowalewski, T.; Holtzman, D. M. *In Situ* Atomic Force Microscopy Study of Alzheimer's β-Amyloid Peptide on Different Substrates: New Insights into Mechanism of β-Sheet Formation. *Proc. Natl. Acad. Sci. U.S.A.* **1999**, *96*, 3688–3693.
34. Zhang, F.; Du, H. N.; Zhang, Z. X.; Ji, L. N.; Li, H. T.; Tang, L.; Wang, H. B.; Fan, C. H.; Xu, H. J.; Zhang, Y.; Hu, J.; Hu, H. Y.; He, J. H. Epitaxial Growth of Peptide Nanofilaments on Inorganic Surfaces: Effects of Interfacial Hydrophobicity/Hydrophilicity. *Angew. Chem., Int. Ed.* **2006**, *45*, 3611–3613.
35. Li, H.; Zhang, F.; Zhang, Y.; Ye, M.; Zhou, B.; Tang, Y. Z.; Yang, H. J.; Xie, M. Y.; Chen, S. F.; He, J. H.; Fang, H. P.; Hu, J. Peptide Diffusion and Self-Assembly in Ambient Water Nanofilm on Mica Surface. *J. Phys. Chem. B* **2009**, *113*, 8795–8799.
36. Kocisko, D. A.; Come, J. H.; Priola, S. A.; Chesebro, B.; Raymond, G. J.; Lansbury, P. T.; Caughey, B. Cell-Free Formation of Protease-Resistant Prion Protein. *Nature* **1994**, *370*, 471–474.
37. Yang, H.; Fung, S. Y.; Pritzker, M.; Chen, P. Surface-Assisted Assembly of an Ionic-Complementary Peptide: Controllable Growth of Nanofibers. *J. Am. Chem. Soc.* **2007**, *129*, 12200–12210.
38. Hooks, D. E.; Fritz, T.; Ward, M. D. Epitaxy and Molecular Organization on Solid Substrates. *Adv. Mater.* **2001**, *13*, 227–241.
39. Tian, B. Z.; Xie, P.; Kempa, T. J.; Bell, D. C.; Lieber, C. M. Single-Crystalline Kinked Semiconductor Nanowire Superstructures. *Angew. Chem., Int. Ed.* **2008**, *47*, 4397–4400.
40. Vettiger, P.; Cross, G.; Despont, M.; Drechsler, U.; Durig, U.; Gotsmann, B.; Haberle, W.; Lantz, M. A.; Rothuizen, H. E.; Stutz, R.; Binnig, G. K. The "Millipede"—Nanotechnology Entering Data Storage. *IEEE Trans. Nanotechnol.* **2002**, *1*, 39–55.
41. An, H. J.; Guo, Y. C.; Zhang, X. D.; Zhang, Y.; Hu, J. Nanodissection of Single- and Double-Stranded DNA by Atomic Force Microscopy. *J. Nanosci. Nanotechnol.* **2005**, *5*, 1656–1659.